BHUTAN HydroMet Journal

National Centre for Hydrology and Meteorology
Royal Government of Bhutan
Thimphu: Bhutan

March 2022

Volume: 1 No.1/2022

Bhutan Hydro-Met Journal, March 2022

Published by National Centre for Hydrology and Meteorology

Address: Doeboom Lam,

Thimphu: Bhutan

P.O. Box No: 207

Website: www.nchm.gov.bt

Tel. No.: +975-2-327202

Fax No.: +975-2-327202

Editorial

Bhutan Hydro-met Journal (BHJ) started in 2022 by National Centre for Hydrology and Meteorology (NCHM) with the objective to promote a culture of research for understanding sciences of hydrology, meteorology and cryosphere in Bhutan. It is our hope that this journal would provide a forum for researchers in the Centre and outside to publish their research works to facilitate dissemination of the results of the studies and research to wider audiences.

This first volume of the journal was launched by Dasho Sonam P Wangdi, Chairman, NCHM Governing Board during the 8th Governing Board meeting of the Centre held on 28th June 2022.

Bhutan HydroMet Journal is an open access journal that will be published annually by NCHM. We are also keeping the publication of relevant articles in this journal open to scientists, researchers, students and other individuals outside of our Centre to meet the objective of this journal.

Exchange and dissemination of information plays an important role in the scientific community. We understand that there are various scientific works done in Bhutan in the field of HydroMet science. It is important that we share the findings from such works with the scientific communities both within and outside of our country. We hope that "Bhutan HydroMet Journal" can contribute in such process of sharing and dissemination of information.

On behalf of the Editorial Committee, I would like to acknowledge and thank Director and the Management of NCHM for their support and assistance. I would also like to thank members of the Editorial Committee for sparing your valuable time reviewing and editing the articles. Lastly I would also like to acknowledge the support, cooperation and contribution received from the officials of NCHM in form of scientific articles, designing and layout of the journal.

Karma Toeb

CONTENTS

National Centre for Medium Range Weather Forecast Unified Model (NCUM) Forecast Verification for Bhutan using simple statistical methods

Monju Subba[1], Saroj Acharya[1] ,Singay Dorji[2]

[1] Engineer, Weather and Climate Services Division, National Centre for Hydrology and Meteorology

[2] Specialist, Weather and Climate Services Division, National Centre for Hydrology and Meteorology

Correspondence e-mail: *msubba@nchm.gov.bt/sacharya@nchm.gov.bt/sdorji@nchm.gov.bt*

Abstract. This article verifies the temperature (maximum and minimum) and rainfall forecasts of National Centre for Medium Range Weather Forecast Unified Model (NCUM) for a selected Class A station for 2021. NCUM is a global deterministic numerical weather prediction model that generates real-time medium-range (10 days) forecast. National Centre for Hydrology and Meteorology prepares the Medium Range Weather Forecast (MRWF) for the country using the NCUM precipitation and temperature forecast. The statistics used for the verification in this study include ME (ME), Root Mean Square Error (RMSE), and correlation coefficient for temperature and Bias, Probability of Detection (POD), False Alarm Ratio (FAR), Hanssen & Kuiper's skill (KSS), and Heidke skill score (HSS) for rainfall event.

The model performs well at forecasting maximum and minimum temperature forecast with some bias. The root mean square error for the majority of the station is found to be increasing with lead time. Overall, the model exhibits a good correlation with the observation, ranging from 0.6 to 0.9. Based on the rainfall data that revealed a score of 0.3-0.7 for KSS and HSS indicating the

accuracy of the model for rainfall events is 30-70 percent. It measures the ability of the forecast to distinguish between occurrence and non-occurrence of the event. It ranges from -1 to 1, 1 being perfect score and 0 as no skill level (WMO, 2014).

Keywords: Medium Range Weather Forecast, NCUM, Forecast Verification, Mean Error, Root Mean Square Error, KSS and HSS.

1. Introduction

National Center for Hydrology and Meteorology (NCHM) provides daily, three-day, and sub seasonal to seasonal weather forecasts. NCHM uses the Environmental Modeling System Weather Research and Forecasting (EMSWRF) model for short-range forecasting, which has an accuracy of 30-50 percent for rainfall events (NCHM, 2019) and (NCHM, 2020). With the growing demand for Medium Range Weather Forecasting (MRWF) across numerous climate and weather user sectors in Bhutan, the center began piloting MRWF in 2020. The center provides Temperature (Maximum and Minimum) and Rainfall forecast for up to 240 hours (up to 10 days) under MRWF.

MRWF for Bhutan is prepared with the support from the National Centre for Medium Range Weather Forecasting (NCMRWF), Government of India. National Centre for Medium Range Weather forecast Unified Model (NCUM) has been used for medium-range weather prediction at NCMRWF since 2012. The information generated from NCUM is also used as a guidance by the regular forecaster to provide early meteorological advisory and warning services. As such there is a need to understand the performance of the NCUM to provide a reliable and accurate medium range forecast. There are two types of weather forecast verification methods; continuous and categorical. Continuous predictands are those elements where a specific value or range of values is forecast and categorical predictands anticipate the occurrence of the event (Stanski, Wilson, & Burrows, 1989). In this study, temperature is subjected to continuous variable analysis, and rainfall is subjected to category variable analysis.

The main objective of this study is to;

- Validate, using simple statistical methods, the accuracy of the NCUM medium range weather forecast for the next 10 days for variables of surface maximum and minimum temperature in degrees Celsius (°C) and the event of rainfall for 2021, by comparing the forecast data with the observation data for the 7 selected Agro meteorological stations (Class A).

- Provide guidance for weather forecasting for variables of surface maximum and minimum temperature and the event of rainfall.
- Check the accuracy and future use of the forecast from the model for the issuance of Medium Range Weather forecasting for the country.

2. Data

2.1. Observed Weather Data

Meteorological variables of surface temperature and rainfall is used for the verification of the NCUM model. There are 20 Agro meteorological stations (Class A) across the country which are identified as the focal point of weather forecasting for Bhutan. For this study, observed temperature data (maximum and minimum) and 24 hours accumulated rainfall data from the 7 selected Class A stations (Fig 1, Table 1) are compared with the forecast data of NCUM for 2021.

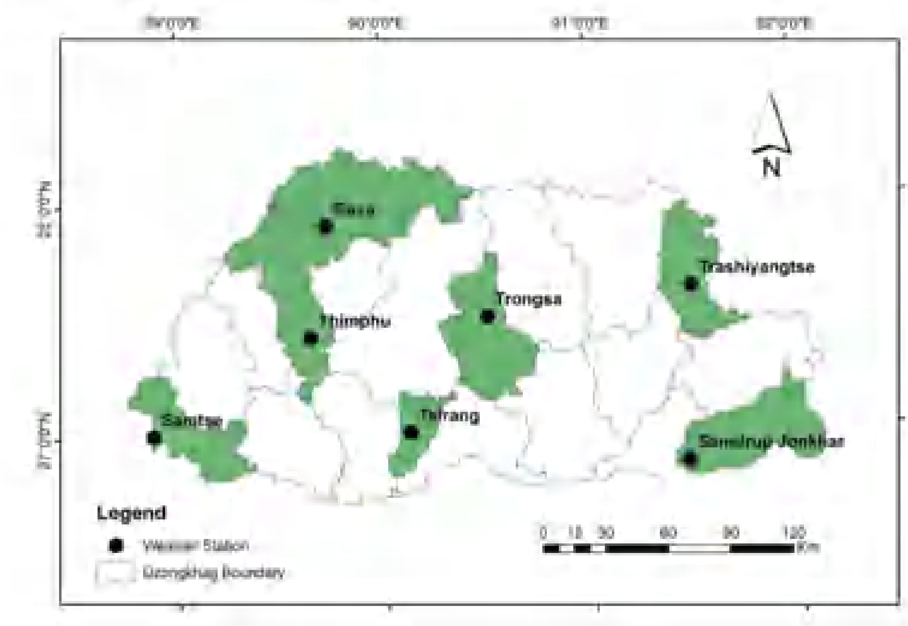

Figure 1*: Location of Selected Agro-met Stations (Class A)*

Table 1 *: Details of selected station location*

Station Name	Latitude (N)	Longitude (E)	Elevation (m)
Samtse	27.02	88.87	550
Tsirang	27.00	90.12	1520
Samdrup Jonkhar	26.86	91.47	300
Gasa	27.90	89.72	2760
Thimphu	27.44	89.68	2310

Trongsa	27.5037	90.5055	2120
Tashi Yangtse	27.6137	91.4977	1830

2.2. NCUM

National Centre for Medium Range Weather Forecast Unified Model (NCUM) is a global Numerical Weather Prediction which is used for generating 10-day numerical weather forecasts routinely since 2012. The model has a resolution of approximately 12 km in horizontal and 70 levels in the vertical reaching 80 km height. NCUM system consists of components for observation pre-processing, observation processing and quality control, data assimilation, forecast model and tools for post processing (Kumar, et al., 2020). An advanced data assimilation method of Hybrid 4D-Var is used for the creation of NCUM global analysis. Data assimilation techniques provide the best estimate of the state of a physical system by combining the information from model and observations to provide an estimate of the state of the system which is better than could be obtained using just the data or the model alone (Daley, 1992). The “hybrid 4D-Var” data assimilation system in the NCUM (Version 6) system is improved with capabilities to assimilate cloud affected microwave radiances from advance microwave sounding unit (AMSU-A) of Advanced Television Infrared Observation Satellite Program (TIROS) Operational Vertical Sounder (ATOVS) instrument (Kumar, et al., 2020). The hybrid technique is scientifically attractive because it effectively integrates the benefits of ensemble data assimilation with the well-known benefits of 4D-Var inside a single data assimilation system (Barker, 2011).

NCUM atmospheric data assimilation system produces analyses at 00, 06, 12 and 18 UTC (Kumar, et al., 2020). NCHM receives 10 days forecast based on

00 UTC analysis and the product are made available at NCHM website and Facebook page. The forecast comprises the expected surface maximum and minimum temperature in degrees Celsius (°C) and rainfall forecast for the next 10 days. Data extraction for the verification of station point was done using Python 3.7 software.

3. Methodology

3.1. Continuous verification of temperature forecasts

Continuous verification scores can provide an overall measure of how the values of the forecasts differ from the observations and the forecast performance. The point forecast is extracted from the grid forecast with the input of latitude and longitude of the observation station. The temperature is averaged and the rainfall is summed to get the daily forecast.

Mean Error, Root Mean Square Error (RMSE) and Correlation Coefficient (CC) are some of the common verification scores categorized under continuous verification approach (Karunasagar et al., 2020) and (Tiriolo et al., 2015)

a) Mean error or bias

It is the average error in a given set of forecasts. It represents a simple and informative score on the behavior of the given variable. If ME >0 (<0), the model exhibits over (under) forecasting. However, it is not an accurate measure as it does not provide information on the manicure of errors. The value ranges from -∞ to +∞. The perfect score is equal to 0.

$$ME = (1/N) \sum (fi - fo) \;\ldots\ldots\ldots\; \textbf{Eq (1)}$$

Where, fi = forecast data, fo = observed data, N= no. of data

b) RMSE

Measures "average" error, weighted according to the square of the error. Does not indicate the direction of the deviations. The *RMSE* puts greater influence on large errors than smaller errors, which may be a good thing if large errors are especially undesirable, but may also encourage conservative forecasting. The value ranges from 0 to +∞. The perfect score is equal to 0.

$$RMSE= (1/N) \sum (fi\text{-}fo)\ \hat{}2 \ldots\ldots\ldots\ \textbf{Eq (2)}$$

Where, fi = forecast data, fo = observed data, N= no. of data

c) Correlation coefficient

CC gives the measure of correspondence between the observations and forecasts. It is a good measure of association or phase error. It varied between -1 to +1; +1 being the perfect score. It must be noted that CC does not take forecast biases in to account.

$$CC = \frac{\sum \quad (fi-f)(Oi-O)}{\sqrt{(fi-f)2}\sqrt{(Oi-O)2}} \ldots\ldots\ldots\ \textbf{Eq (3)}$$

Where, fi = forecast value, f= forecast mean value, fo =observed value, O=observed mean value

3.2. Categorical verification of rainfall forecasts

We defined the event before creating a dichotomous variable. Defining the event- according to the World Meteorological Organization (WMO, 2014, Table 2), states that the nature of the event must be predicted and must be clearly stated in order to understand what is being predicted and the location.

Accordingly, the contingency table for rainfall is prepared with model run as 'Event Forecast (yes/no)' and observed station rain 'Event Observed (yes/no)' to collect a match set of forecast and observation. As per NCHM rainfall classification, rainy day is defined as day when a station and model records 1 mm or more rainfall in a day.

Table 2*: Contingency table for dichotomous variable analysis* (WMO, 2014)

	Event observed		**Marginal total**
	Yes	**No**	
Event Yes	a	B	a+b
Forecast No	c	D	c+d
Marginal total	a+c	b+d	a+b+c+d

(a=Hit, b=False alarm, c=Miss, d= Correct Rejection)

It is considered an event as a hit (a) when the prediction of an event matches with the observation on a grid point. On the other hand, an event on a grid point is predicted but it is not observed, it is denoted as a false alarm (b). A miss (c) occurs when an event is not predicted but it is actually observed. Finally, correct rejection (d) is when an event does not occur and model does not predict. Based on these components of the contingency table 2, categorical skill scores are computed for different rainfall thresholds.

Table 3 *: Verification scores used for categorical verification* (WMO, 2014)

1	**Frequency Bias (B)**	*Frequency bias= a+b/ (a+c)*

	The frequency bias (B), it refers to as bias, uses only marginal sums of the contingency table. It compares the forecast and observed frequencies of occurrence of the event in the sample. The forecast is said to be unbiased if the event is forecast exactly the same frequency with which it is observed, so that the frequency bias of 1 represents the best score.	*............* ***Eq (4)*** *Where, a=hit, b=false alarm, c=miss.*
2	**Probability Of Detection (PoD) (Hit rate (HR)** The hit rate (HR) has a range of 0-1 with 1 representing a perfect forecast. It uses only the observed events and c in the contingency table and it is sensitive only to missed events and not false alarms. The HR is incomplete by itself, so it is being used in conjunction with either false alarm ratio or false alarm rate.	*PoD=HR=a/(a+c)* *............* ***Eq (5)*** *Where, a=hit, c=miss.*
3	**False Alarm Ratio (FAR)** The false alarm ratio (FAR) is the ratio of the total false alarms (b) to the total events forecast (a+b). It ranges from 0-1, 0 being a perfect score. It is insensitive to missed events. It is also incomplete score, so it should be used in connection with the HR [1].	*FAR= b/(a+b)* *............* ***Eq (6)*** *Where, a=hit, b=false alarm.*
4	**The Heidke Skill Score (HSS)**	*HSS=2(ad-bc)/[(a+c)(c+d)+(a+b)(b+d)]*

	Skill is the accuracy of a forecast compared with the accuracy of a standard forecast. The HSS ranges from negative value to +1	………… ***Eq (7)*** *Where, a=hit, b=false alarm, c=miss, d=correct rejection.*
5	**The Hanssen-Kuipers Score (KSS)** It is the difference between the hit rate and the false alarm rate. It measures the ability of the forecast to distinguish between occurrence and non-occurrence of the event. It ranges from -1 to 1, 1 being perfect score and 0 as no skill level	*KSS=ad-bc/[(a+c)(b+d)]* ………… ***Eq (8)*** *Where, a=hit, b=false alarm, c=miss, d=correct rejection.*

4. Results

4.1. Continuous variable

4.1.1. Maximum Temperature

Based on the analysis of the maximum temperature (Table 4), the bias was negligible for Thimphu for all the forecast days. All the stations were under-predicted except Tsirang and Thimphu. Gasa had the highest under prediction, with a bias of -7.50, followed by Tashiyangtse with an average bias of -6.23, Trongsa with an average bias of -5.00, and Samtse with an average bias of -4.00. Overall, the model has a good correlation with the observation ranging from 0.60 to 0.90 for Bhutan.

Table 4 : ***Mean error and correlation for maximum temperature***

	Mean Error		Correlation	
	Day 1	**Day 10**	**Day 1**	**Day 10**
Samtse	-4.12	-3.77	0.78	0.89
Tsirang	1.41	1.49	0.88	0.81
Samdrup Jonkhar	-0.91	-0.75	0.86	0.62
Gasa	-8.17	-6.91	0.69	0.65
Thimphu	0.13	0.27	0.87	0.77
Trongsa	-4.70	-5.21	0.79	0.76
Tashiyangtse	-6.16	-6.56	0.84	0.79

Figure 2 shows that the RMSE increases with lead time for Thimphu, Trongsa, Tashiyangtse, Samtse and Tsirang station whereas the Gasa station shows decrease in RMSE with lead time. RMSE is higher for Gasa and lower for Tsirang, Samdrup Jonkhar and Thimphu.

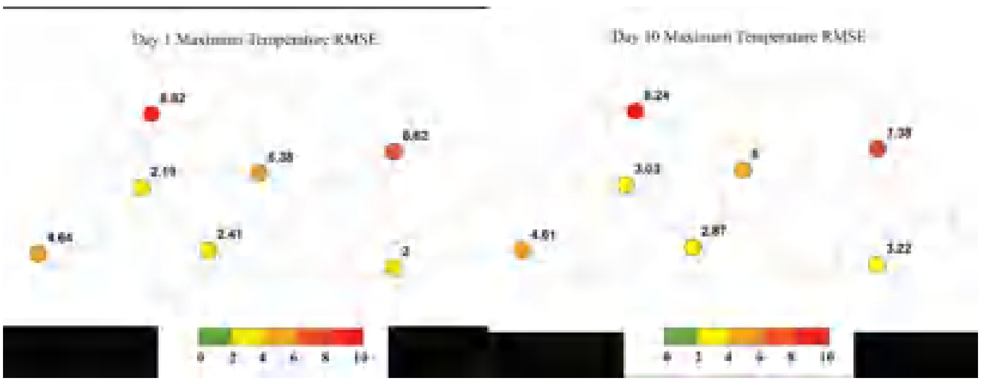

Figure 2: ***Maximum Temperature RMSE of selected class A stations***

4.1.2. Minimum Temperature

The NCUM minimum temperature was under-predicted for most of the station points with the highest average bias of -6.4 in Gasa (Table 5). Tsirang has nearly negligible average bias of -0.03. Overall, the model has an excellent correlation with the observation ranging above 0.9 for Bhutan.

Table 5*: Mean error and correlation for minimum temperature*

	Mean Error		Correlation	
	Day 1	**Day 10**	**Day 1**	**Day 10**
Samtse	-1.26	-0.73	0.97	0.90
Tsirang	0.65	0.53	0.96	0.94
Samdrup Jonkhar	-0.13	0.22	0.97	0.93
Gasa	-6.54	-6.25	0.96	0.92
Thimphu	-1.15	-1.30	0.94	0.92
Trongsa	-4.67	-4.82	0.96	0.95
Tashiyangtse	-2.52	-3.32	0.96	0.94

Figure 3 shows that the RMSE remained almost same for Thimphu for most of the forecast days. Samtse, Samdrup Jonkhar Trongsa and Tashiyangtse showed an increase in RMSE for all forecast days. Whereas Gasa showed increase, then decrease with the lead time.

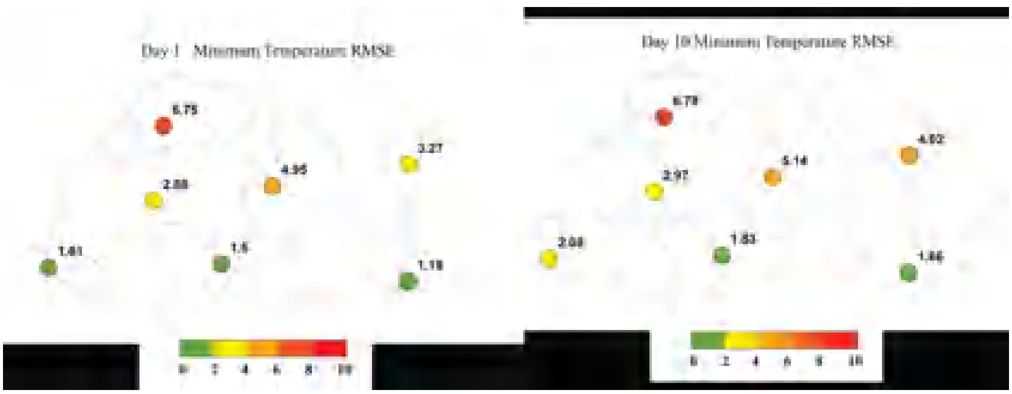

Figure 3*: Minimum Temperature RMSE of selected class A stations*

4.2. Dichotomous variable analysis

Most of the station has frequency bias near to 1 with ± 1 variation showing little difference between forecast and observation except for Thimphu and Tsirang where the variation is greater than 1.

The Probability of Detection (POD), sometimes called Hit rate ranges from 0.7 – 1.0 meaning the forecast was able to capture the event of rainfall 70% to 100% respectively. Thimphu has highest FAR values ranging from 0.6 to 0.75 (Table 6). It indicates that 60% to 75% of the forecast were not observed on the valid forecast period. FAR for the rest of the stations are from 0.3 to 0.6 (Table 6).

Table 6: ***Computed scores for Rainfall***

	Day 1			Day 10		
	B	**POD**	**FAR**	**B**	**POD**	**FAR**
Samtse	1.33	0.88	0.34	1.52	0.96	0.37
Tsirang	1.73	1.00	0.42	2.13	0.94	0.56
Samdrup Jonkhar	1.84	0.95	0.49	1.42	0.95	0.33
Gasa	1.23	0.80	0.35	0.90	0.74	0.18
Thimphu	3.73	1.00	0.73	3.09	0.82	0.74
Trongsa	1.62	0.86	0.47	1.35	0.85	0.37
Tashiyangtse	1.57	0.86	0.45	1.60	0.80	0.50

The Hanssen & Kuiper's skill (KSS) and Heidke skill score (HSS) for southern region has higher values (>0.4) for all the forecast days suggesting good skill. All the stations have a score between 0.3-0.7 for KSS and HSS. It illustrates that the model has accuracy of 30% to 70% for the rainfall event (Fig 4).

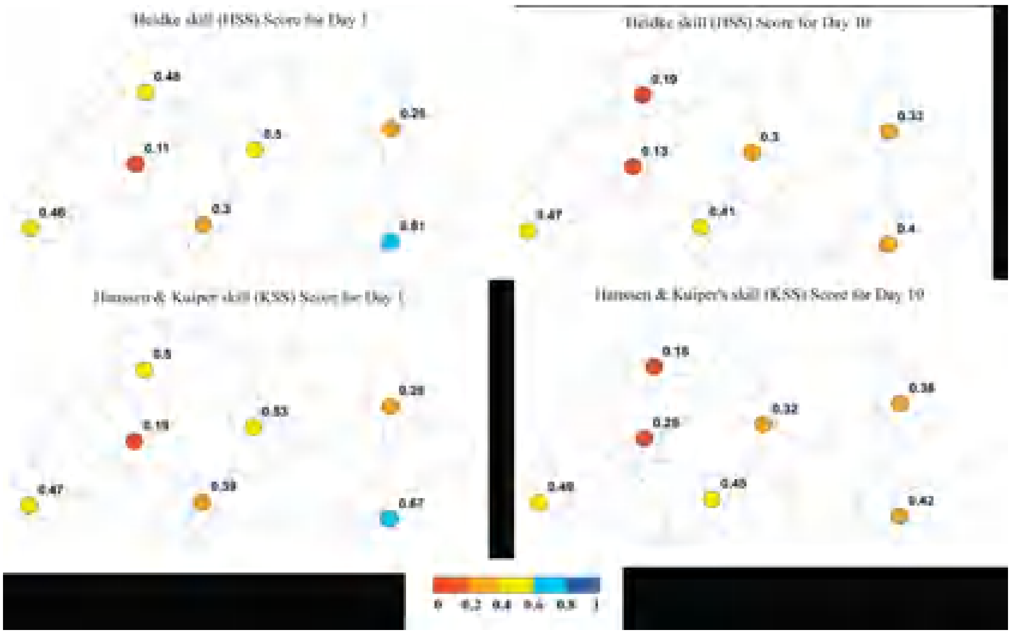

Figure 4*: HSS and KSS score of selected class A stations*

5. Conclusion

This paper shows the verification of NCUM forecast with the observation data from 7 selected station points of the country analyzed for all the 10 days forecast.

Results show that RMSE is 2-8 Degree Celsius for Maximum Temperature and 1-6 Degree Celsius for Minimum Temperature. For both Maximum and Minimum Temperature RMSE is higher for the northern region and lower for southern parts of the country. There was an increase in RMSE with lead time for the majority of the station. Rainfall events were captured well with scores between 0.3-0.7 for KSS and HSS. It illustrates that the model's accuracy for the rainfall event ranges from 30% to 70%. It measures the ability of the forecast to distinguish between occurrence and non-occurrence of the event. Southern stations have higher scores, signifying the model performance to be better in the plains.

The model has performed well in forecasting both temperature and rainfall for the southern regions. The bias was seen to increase with altitude. Statistical bias correction approaches, such as MOS and Kalman filters, are needed for stations with higher RMSE and Bias to enhance medium-range forecast accuracy. The medium range weather forecast would be very helpful for the agriculture sector and other climate sensitive agencies for making effective plans.This information will also aid climate change adaptation planning and to enhance preparedness and response to extreme weather events.

References

Barker, D. (2011). *Data Assimilation – progress and plans.* UK: MOSAC-16.

Daley, R. (1992). Atmospheric Data Analysis. *American Meteorological Society, 73*, 1050-1052. Retrieved from https://www.jstor.org/stable/26229644

Karunasagar, S., Sharma, K., Kumar, S., & Ashrit, R. (2020). *MoES Model Forecast Verification during JJAS2019: Verification of Rainfall Forecasts*. Noida, India: National Center for Medium Range Weather Forecast .

Kumar, S., Bushair, M. T., Prakash, B., Lodh, A., Sharma, P., George, G., Rajagopal, E. N. (2020). *NCUM Global NWP System: Version 6 (NCUM-G:V6).* Noida, India: National Centre for Medium Range Weather Forecast.

NCHM. (2019). *Report on WRF verification.* Thimphu: NCHM.

NCHM. (2020). *Report on WRF verification.* Thimphu,Bhutan: NCHM.

Stanski, H. R., Wilson, L. J., & Burrows, W. R. (1989). *Survey of common verification methods in meteorology.* Canada: Atmospheric Environment Service.

Tiriolo, L., Torcasio, R. C., Montesanti, S., & Federico, S. (2015). Verification of a Real Time Weather Forecasting System in Southern Italy. *Advances in Meteorology, vol.2015*. Retrieved from https://doi.org/10.1155/2015/758250

World Meteorological Organization. (2014). *Forecast Verification for African Severe Weather Forecasting: Demonstration Projects.* Geneva, Switzerland: World Meteorological Organization.

Comparison of Mass Balance Values between Glaciological and in-situ Geodetic Method as revealed from the observations on two benchmark glaciers – *Gangju La and Thana Glacier, Bhutan Himalaya*

Phuntsho Tshering[1], Karma Toeb[2]

[1] Executive Geologist, Cryosphere Services Division, National Center for Hydrology and Meteorology

[2] Specialist, Cryosphere Services Division, National Center for Hydrology and Meteorology

Correspondence e-mail: ptshering@nchm.gov.bt/karma@nchm.gov.bt

Keywords: Glacier, glacier mass balance, glaciological method, *in-situ* geodetic method, snow and ice density

Abstract. Glaciers worldwide are losing their masses drastically due to climate change and other factors and the Himalayan glaciers are not an exception. Two benchmark glaciers in Bhutan Himalaya are monitored every year using glaciological and *in-situ* geodetic methods. The mass balance values on two glaciers using glaciological and *in-situ* geodetic methods are compared for the survey periods having mass balance values for both the methods, Gangju La glacier reveals the difference as low as 10 m w.e.a^{-1} (2013 – 2014) to as high as 2010 m w.e.a^{-1} (2012 – 2013). In case of Thana glacier, there are three survey periods having the mass balance values for both the methods and reveals the differences ranging from 265 m w.e.a^{-1} (2019 – 2020) to as high as 300 m w.e.a^{-1} (2016-2017). On both the glaciers it reveals that the mass balance values obtained through *in-situ* geodetic method are more negative than the values using glaciological method. Unlike the glaciological method which measures only the surface changes, the in situ geodetic method of measuring mass balance has the ability to detect and

take into account the internal mass changes taking place within the glacier. Therefore, the higher negative mass balance values (greater mass loss) shown by *in-situ* geodetic method can be attributed to such aspect of the method. The study does not capture any bias and errors regarding different methodologies applied.

1. Introduction

Glaciers worldwide started losing their masses drastically over the last century contributing to global sea-level rise. Himalayan glaciers, covering 33,000 km^2 by area (Schenck & Uestion, 2012) spanning over eight countries across Asia, are considered to be the third pole and not an exception and revealed an accelerated mass loss (Lee et al., 2021). Glacier mass balance observations are crucial in the context of climate change, water resources, and global sea-level rise. Glacier mass balance can be measured either by glaciological (direct) or geodetic methods (Cogley, 2009; Zemp et al., 2009) in order to understand the hydrological behaviors and survival of the glaciers with climate change. Attempts to study glaciers regarding mass balance in the Bhutan Himalayas were initiated in recent years not spanning over 20 years.

The glaciological method involves establishment of *in-situ* measurement stakes over the glacier surface measuring accumulation and ablation and interpolating measurements across the glacier surface whereas the geodetic method is based on repeated measurements of glacier surface elevation using consecutive digital elevation models (DEM) developed from either field surveys, aerial or spaceborne data (Cogley, 2009; Zemp et al., 2009). The conventional glaciological method measures only the surface mass balance (SMB) depending on the number of observation points installed over the glacier surface whereas the geodetic method incorporates the changes that occurred over the entire glacier including surface, internal and basal changes over the observation period. In the recent times, both the methods are practiced world-wide to compare the mass balance values and often, the mass balance values obtained through geodetic methods are used to calibrate the glaciological method. The advantage of geodetic method is that the mass balance of a particular glacier can be estimated for multi-annual resolution whereas glaciological can be annual.

The first-ever glacier mass balance observations in Bhutan Himalayas were started in 2003 by a group of Japanese experts in collaboration with the Department of Geology and Mines, Ministry of Economic Affairs (the then Ministry of Trade and Industry). Measurement stakes were installed on the Gangju La glacier and the data were retrieved in the following year. *In-situ* geodetic measurement was also initiated in 2004 by setting up benchmarks near the glaciers for post-processing of the geodetic data. The observation on Gangju La glacier resumed from 2011 through a collaborative project (DGM-JICA/JST project) and since then, continuous monitoring has been conducted using both methods. However, the glaciological method on the Gangju La glacier was done away due to the disturbances by the trespassers and sustainability issue of the measurement stakes. The available data retrieved using glaciological methods were analyzed and reported by Tshering and Fujita, 2012. In recent years, similar studies were also initiated on the Thana glacier in the headwater of Chamkhar Chhu. Since then, the observations on the glacier using both glaciological and geodetic (*in-situ*) methods are being continued.

The aim of this article is to compare the glacier mass balance values between glaciological and geodetic methods using available data sets on two benchmark glaciers of Bhutan (Gangju La and Thana glaciers). Although the glaciological and geodetic methods measure the net glacier-wide balance of the same glacier, the difference in value may firstly vary due to the methods deployed, secondly due to the inability to incorporate internal changes for glaciological methods and quality of DEM generated in case of geodetic methods. Over the years, such outcomes of the comparison can be used to calibrate the mass balance values obtained through glaciological method.

2. Study Area and earlier works

Figure 1 shows the location map of benchmark glaciers of Bhutan. Gangju La glacier (27.940°N, 89.950°E) in the headwater of Pho Chhu. It has an area of less than a km^2. Initial stakes were installed over Gangju La glacier in 2003 and the change in glacier surface elevation change (stake height) were retrieved in 2004 along with stake positions (latitude, longitude and elevation) using a theodolite with laser distance finder (Tshering & Fujita, 2016). Similarly, mass balance data through installation of stakes (glaciological method) were collected for survey periods (2012 – 13 and 2013 – 14) during which, the stake locations were picked up using Promark 3, Megellan GEM-1, GNSS Technologies, Inc. The geodetic method was initiated in 2004 and mapped the glacier surface elevation using the carrier-phase differential GPS (dGPS) and continued in 2011, 2012, 2013, and 2014 using using Promark 3, Megellan GEM-1, GNSS Technologies, Inc. The results were published in Annals of glaciology (Tshering and Fujita, 2016). From 2017 the Cryosphere Services Division under the National Centre for Hydrology and Meteorology has included mass balance work of Gangju La glacier as a part of annual cryosphere monitoring program for collection of long-term data and information for understanding cryosphere in Bhutan. Annual field survey data are analyzed and mass balance values are archived and as well as published in the form of scientific reports.

Thana glacier (28.016°N, 90.613°E) is also a clean-type glacier in the headwater of Chamkhar Chhu. It has an area of more than 3 km^2. Mass balance monitoring of glacier started in 2012, but the reliable data sets were obtained only after 2016 field survey. Thana glacier also another benchmark of Bhutan that is being monitored as a part of annual cryosphere monitoring program by the Cryosphere Services Division. All the field survey data and analysis are archived and published in the from scientific reports.

Glaciers in Nepal and Bhutan lie in the eastern part of the Himalayas. The region falls under intense summer monsoon which also is identified as major source of nourishment for the glaciers. This is the reason why glaciers in eastern part of the Himalayas are also called "summer accumulation type" (Y. Ageta; K. Higuchi, 1984).

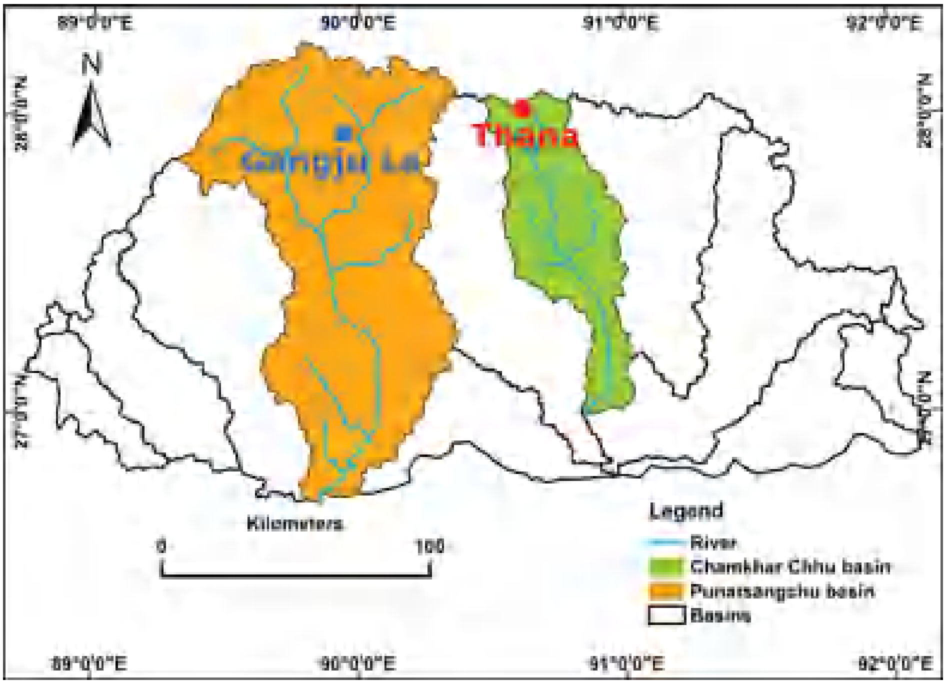

Figure 1: Location maps of two benchmark glaciers of Bhutan, Gangju La and Thana glacier (Tshering, 2021).

3. Methodology

The following section describes the measurement methods on how the mass balance data were acquired, equipment used and formulae used for estimating the mass balance on both the benchmark glaciers.

3.1. Glaciological method

3.1.1. Data acquisition

Bhutanese glaciers are located towards the eastern part of the Himalaya and are located at very high elevations with rugged terrain. Owing to the logistical and accessibility constraints, the glaciers in Bhutan can be accessed only once in a year during Autumn season (September – November) of the year. During summer, it receives heavy snow and it is merely impossible for carrying out survey. Stakes were installed over the glacier surface (Figure 2) covering elevation gradients (e.g., longer stake intervals having even elevation gradient and shorter stake intervals having sudden elevation gradient change). While retrieving the stake data, the stake height changes above the ice surface between the previous and following balance years were measured (Table 1). The locations (latitude, longitude and elevation) of the stakes were also picked up using global positioning system (GPS) as shown in table 1.

Table 1: Detailed stake installation information on Thana glacier during installation (2017) and retrieving of data (2018). Stake ID shows the take numbering

Stake ID	**Stake Height above ice** (cm)		**Latitude** (decimal degree)	**Longitude** (decimal degree)	**Elevation** (m a.s.l.)
	Installation (2017)	Recovery (2018)			
70-16	360.0	400.8	28.031669617	90.600752589	5541.41

58-17	52.5	289.0	28.027466530	90.606970017	5317.97
55-17	98.0	350.0	28.025357028	90.604965237	5362.01
45-16	172.0	465.0	28.025080628	90.607910573	5298.17
28-16	186.8	343.0	28.022902194	90.611015071	5274.80
27-16	236.0	568.0	28.019765715	90.611958122	5257.83
26-17	73.6	380.0	28.017061267	90.613386966	5231.24
24-17	59.3	400.0	28.014479416	90.613541125	5219.28
22-17	76.5	398.0	28.011997224	90.613356075	5209.39
20-17	63.5	480.0	28.013106957	90.616552603	5206.50
19-17	46.0	494.0	28.013922803	90.618354943	5181.16

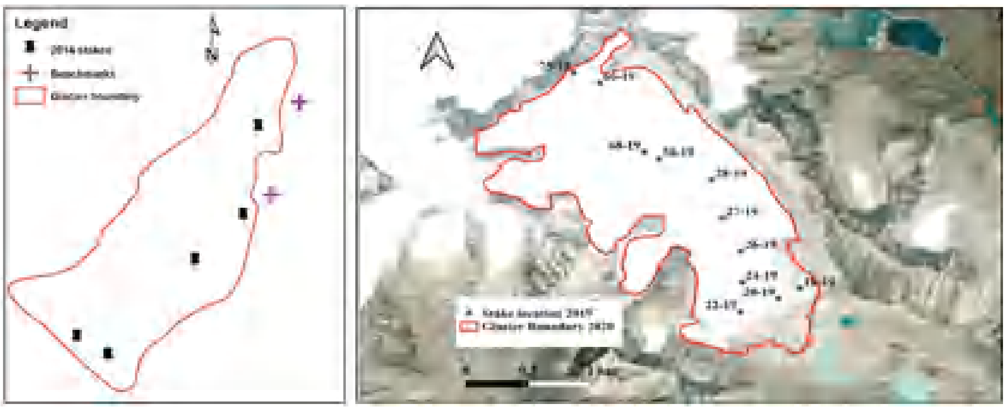

Figure 2: Stake locations on two benchmark glaciers. Left: Gangju La glacier (2014) and Right: Thana glacier (2019)

3.1.2. Mass balance calculation

The glaciological annual mass balance was calculated by formulating the changes in stake height (glacier ice thickness change) incorporating changes in snow thickness. The specific mass balance at a point was calculated using equation (i), following Tshering and Fujita, 2016:

$$b_d = \frac{\Delta h_d \rho_i + (S_{t2} - S_{t1})(\rho_s - \rho_i)}{(t_2 - t_1)} \quad \text{......................} \text{ (i)}$$

Where b_d is the annual mass balance at a given point by the glaciological method (kg m^{-2} a^{-1} equivalent to mm w.e.a^{-1}); Δh_d is the difference in stake height (m) between years t1 and t2 and it is negative when the glacier surface lowers; ρ_s and ρ_i are density of snow and ice (kg m^{-3}) respectively. The density of snow was considered 488.8 kg m^{-3} (calculated from snow pit analysis) in elevations having snow more than 1 m thickness and 400 kg m^{-3} in places having snow less than 1 m thickness. The density of ice was assumed 880 kg m^{-3}. S_{t2} and S_{t1} are thickness of snow (m) for years t2 and t1 respectively. Snow thickness were measured at the stake locations and the snow pit measurement was carried out near the upper most stake (in case of Thana glacier). The thickness of the snow for consecutive survey years at respective elevation bands were estimated from the linear regression fit (Figure 3, left). The representative specific mass balance at each 50 m elevation bands were picked up from the linear regression fit (Figure 3, right), and thus obtained the mass balance at each 50 m altitude band ($\overline{b_{dz}}$; mm w.e.a^{-1}).

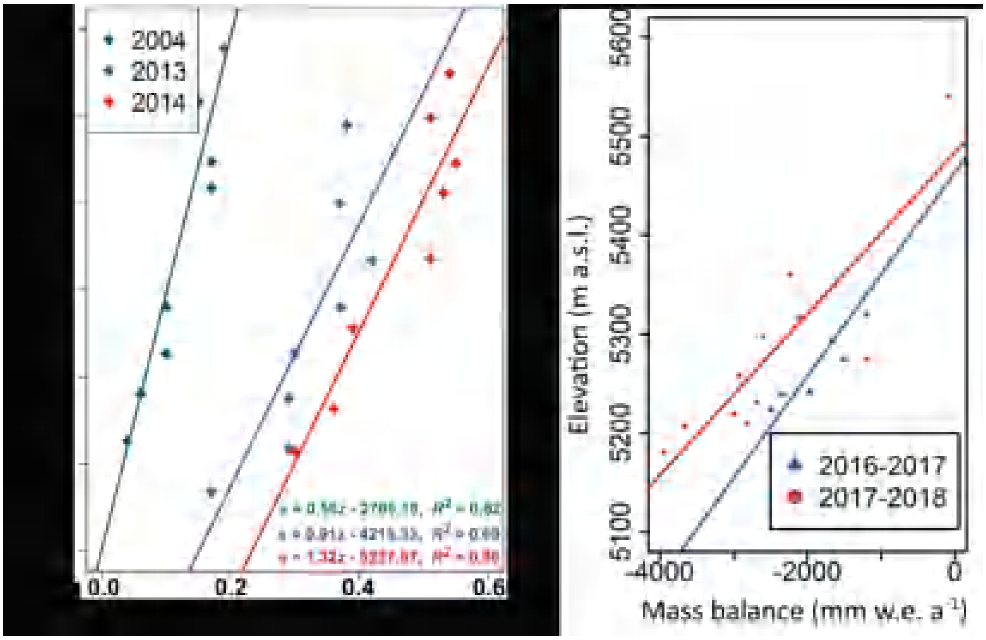

Figure 3: Left: Linear regression graphs of snow thickness (m) along the profile on Gangju La glacier and; Right: An example of glacier mass balance linear regression from Thana glacier for two years

The area-averaged annual mass balance ($\overline{b_d}$; mm w.e.a^{-1}) were then obtained from equation (ii)

$$\overline{b_d} = \frac{\Sigma_z A_z b_{dz}}{A_T} \text{ .... (ii)}$$

Where A_z and A_T are glacier area within 50 m altitude band and total area (m^2) respectively. b_{dz} is the average mass balance within 50 m altitude band. The glacier surface area was extracted using available high resolution DEMs. The area (A_z) of each 50 m altitude band was then extracted from the same. An example of stake data acquisition from Thana glacier for one survey year (2017 – 2018) is given in table 1.

3.2. Geodetic (*in-situ*) method

3.2.1. Data acquisition

Himalayan glaciers as a whole are widely accessed in terms of glacier mass balance using remotely sensed satellite imageries known as geodetic method. It is mainly due to the inaccessibility to the site and harsh weather conditions. Among such studies, the *in-situ* based geodetic methods are also proved successful (e.g., Tshering and Fujita, 2016; (Fujita & Nuimura, 2011); (Azam et al., 2018)). In the earlier survey periods, *in-situ* geodetic surveys were conducted using different global positioning system (dGPS), Spectra Precision Promark 180™. Such system requires at least two accurate temporary benchmarks (TBM) for post processing of the data. During the survey, one dGPS equipment is set as a base station (static mode) and two or more equipment are set as rover (kinematic mode), backpacked and then walked rigorously on the glacier surface to get the surface elevation data (Fig. 4). In the recent times, Trimble GNSS system which has real time kinematic (RTK) functions were used. The base was set on a known point and rovers were then backpacked and walked on the glacier surface to get the elevation data. In case of Gangju La glacier, due to its easy accessibility, almost entire glacier surface was mapped whereas for Thana glacier, only parts of the accessible parts were mapped. The data sets were then exported to CSV format for further processing.

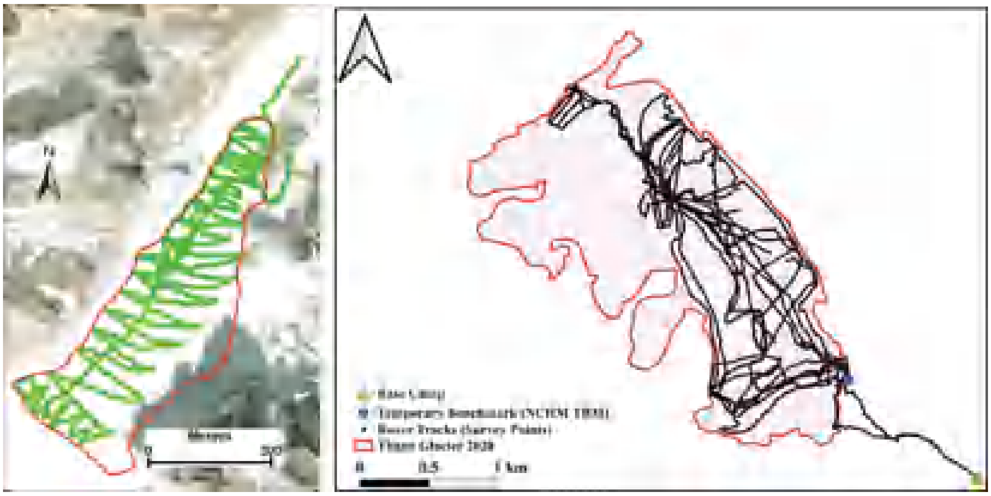

Figure 4: The red polygon on both the images shows the glacier boundaries. The green track on the left figure shows the dGPS tracks of 2020 on Gangju La glacier and the black tracks on right figure shows the dGPS tracks on Thana glacier of 2020

3.2.2. Data post processing and mass balance calculation

The CSV format data were then post processed using GNSS solution software and then DEMs of 1m resolutions were generated along the survey tracks in ArcGIS platform. The DEMs of two subsequent survey years were then compared and differenced to get the elevation changes of the glacier surface between two successive years (fig. 5)

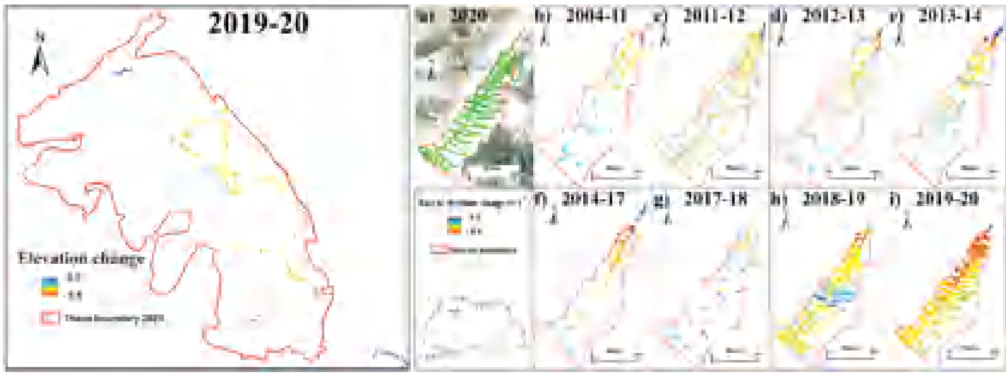

Figure 5: Surface elevation change map of Gangju La glacier. Right: a) dGPS tracks. b – e; are the surface elevation change reproduced from Tshering and Fujita 2016 and f – i are the surface elevation change through in-situ geodetic

survey. Left: Surface elevation change map of Thana glacier for survey year 2019 – 20

Several elevation changes falling within every 50 m elevation bands were averaged to get a single representative elevation change within the particular elevation band. The annual mass balance (geodetic) at a point is calculated using equation (iii) of Tshering & Fujita, 2016 as follows:

$$b_g = \frac{\Delta h_g \rho_i + (S_{t2} - S_{t1})(\rho_s - \rho_i)}{(t_2 - t_1)} \text{ .... (iii)}$$

Where b_g is the annual mass balance at a given point by the geodetic method (kg m^{-2} a^{-1} equivalent to mm w.e.a^{-1}); Δh_g is the surface elevation change between years t1 and t2 (m); ρ_s and ρ_i are density of snow and ice (kg m^{-3}) respectively. S_{t2} and S_{t1} are thickness of snow (m) for years t1 and t2.

Finally, the area-averaged annual mass balance (b_g; mm w.e.a^{-1}) was estimated using equation (iv) as follows:

$$\overline{b_g} = \frac{\Sigma_z A_z b_{gz}}{A_T} \text{ .... (iv)}$$

Where A_z and A_T are glacier area within 50 m altitude band and total area (m^2) respectively. b_{dz} is the average mass balance within 50 m altitude band. The glacier surface area was extracted using available high resolution DEMs and in some years, surface area DEM was generated using the field survey dGPS track points. The area (A_z) of each 50 m altitude band was then extracted from the same.

4. Results and Discussion

Table 2 shows the mass balance values of Gangju La and Thana glaciers obtained through glaciological and geodetic (*in-situ*) method spanning over almost two decades for Gangju La and less than a decade for Thana glacier. Comparing the available mass balance values for both the glaciers, it reveals that the mass balance through glaciological method is less negative and more negative for geodetic (*in-situ*) method. The uncertainty values were assessed following Tshering and Fujita, 2016.

Table 2: Mass balance values of two benchmark glaciers of Bhutan used in this study.

Year	**Gangju La (mm w.e. a^{-1})**		**Thana (mm w.e. a^{-1})**	
	Direct	**Geodetic**	**Direct**	**Geodetic**
2003 – 04	-1230±230	–	–	–
2004 – 11	–	-1790±260	–	–
2011 – 12	–	-2040±460	–	–
2012 – 13	-1810±160	-2020±290	–	–
2013 – 14	-1110±160	-1120±310	–	–
2014 – 17	–	-1350	–	–
2016 – 17	–	–	-660	-930
2017 – 18	–	-2390	-1570	-1870
2018 – 19	–	1470	-1650	–
2019 – 20	–	1660	-2645	-2910

The advantage of conducting glaciological method for the two benchmark glaciers is that they are not so large in terms of area and the measurement stakes can be easily installed over the entire glacier surface. The glaciological method measures only the surface mass balance and it is unable to capture mass changes occurring within the glacier. For instance, glacier may either gain mass internally due to freezing of water bodies flowing through an englacial channel or losing mass due to basal melting and ablation. In such scenarios, the *in-situ* geodetic method can capture the overall changes that occurs to a glacier (surface, internal, basal) be it an accumulation or ablation. (Cox & March, 2004) have compared the mass balance values of Gulkana glacier, Alaska, USA and found that ignoring an internal ablation which is captured in geodetic method would decrease the cumulative glaciological balance by about 10%. However, the mass balance values acquired through geodetic method depends on the quality of DEM and topographic maps and have suggested that the errors related to geodetic balance may account for larger errors. From other studies, internal ablation contributed to the overall thinning of some glacier as high as 0.16 m w.e.a^{-1} (Andreassen et al., 2016). Our benchmark glaciers are located morphologically on a slopy landscape and sliding downward at a higher velocity than others in the region. Under such conditions the potential energy loss by the transfer of mass towards down-slope leads to more internal strain heating and frictional warming at the bed (Thomson et al., 2017). Such phenomena could have contributed to the internal ablation and hence, exhibiting more mass loss by in-situ geodetic method.

5. Conclusion

The study compared the glacier mass balance values of two benchmark glaciers of Bhutan for glaciological and in-situ geodetic methods. Table 2 shows the available mass balance values for the entire survey periods. For the survey periods having mass balance values for both the methods, Gangju La glacier reveals the difference of as low as 10 m w.e.a^{-1} (2013 – 2014) to as high as 2010 m w.e.a^{-1} (2012 – 2013). In case of Thana glacier, there are three survey periods having the mass balance values for both the methods and reveals the differences ranging from 265 m w.e.a^{-1} (2019 – 2020) to as high as 300 m w.e.a^{-1} (2016-2017). Both the glaciers reveals that the *in-situ* geodetic method shows greater mass loss than that by glaciological method. However, the study does not capture any bias and errors regarding different methodologies applied. Therefore, the following conclusion are drawn from the study:

- Both the methods are simultaneously practiced world-wide and in the absence of literatures on which method is better, it is timely that the mass balance values obtained through glaciological methods be corrected and calibrated using mass balance values of geodetic method.

- For future water budget studies, the geodetic method is recommended as it reveals overall changes of the glacier whereas the glaciological method captures only the surface changes.
- If the glacier is not annually visited for field survey, the geodetic method for mass balance studies is recommended as the changes on the glacier can be calculated even after decades.

References

Andreassen, L. M., Elvehøy, H., Kjøllmoen, B., & Engeset, R. V. (2016). Reanalysis of long-term series of glaciological and geodetic mass balance for 10 Norwegian glaciers. *Cryosphere*, *10*(2), 535–552. https://doi.org/10.5194/tc-10-535-2016

Azam, M. F., Wagnon, P., Berthier, E., Vincent, C., Fujita, K., & Kargel, J. S. (2018). Review of the status and mass changes of Himalayan-Karakoram glaciers. *Journal of Glaciology*, *64*(243), 61–74. https://doi.org/10.1017/jog.2017.86

Cogley, J. G. (2009). Geodetic and direct mass-balance measurements: Comparison and joint analysis. *Annals of Glaciology*, *50*(50), 96–100. https://doi.org/10.3189/172756409787769744

Cox, L. H., & March, R. S. (2004). Comparison of geodetic and glaciological mass-balance techniques, Gulkana Glacier, Alaska, U.S.A. *Journal of Glaciology*, *50*(170), 363–370. https://doi.org/10.3189/172756504781829855

Fujita, K., & Nuimura, T. (2011). Spatially heterogeneous wastage of Himalayan glaciers. *Proceedings of the National Academy of Sciences of the United States of America*, *108*(34), 14011–14014. https://doi.org/10.1073/pnas.1106242108

Lee, E., Carrivick, J. L., Quincey, D. J., Cook, S. J., James, W. H. M., & Brown, L. E. (2021). Accelerated mass loss of Himalayan glaciers since the Little Ice Age. *Scientific Reports*, *11*(1), 1–8. https://doi.org/10.1038/s41598-021-03805-8

Schenck, R., & Uestion, Q. (2012). *Ees 717 : E Arth S Ystem S Cience Ii T*

Ake - Home M Idterm R Esponses To. *58*.

Thomson, L. I., Zemp, M., Copland, L., Cogley, J. G., & Ecclestone, M. A. (2017). Comparison of geodetic and glaciological mass budgets for White Glacier, Axel Heiberg Island, Canada. *Journal of Glaciology*, *63*(237), 55–66. https://doi.org/10.1017/jog.2016.112

Tshering, P. (2021). Mass Balance Status of Glaciers of Bhutan Himalayas As observed on Gangju La and Thana. *Cryosphere Services Division, National Center for Hydrology and Meteorology, Bhutan*.

Tshering, P., & Fujita, K. (2016). First in situ record of decadal glacier mass balance (2003–2014) from the Bhutan Himalaya. *Annals of Glaciology*, *57*(71), 289–294. https://doi.org/10.3189/2016aog71a036

Y. Ageta; K. Higuchi. (1984). *Estimation of Mass Balance Components of a Summer-Accumulation Type Glacier in the Nepal Himalaya*. 249–255. http://www.jstor.org/

Zemp, M., Hoelzle, M., & Haeberli, W. (2009). Six decades of glacier mass-balance observations: A review of the worldwide monitoring network. *Annals of Glaciology*, *50*(50), 101–111. https://doi.org/10.3189/172756409787769591

River Flow Trend and Flood Frequency Analysis of Punatsangchhu River

Chimi Namgyel[1], Tayba Buddha Tamang[2]

[1] Senior Statistical Officer, Hydrology and Water Resources Services Division, National Center for Hydrology and Meteorology

[2] Chief, Hydrology and Water Resources Services Division, National Center for Hydrology and Meteorology

Correspondence email: cnamgyal@nchm.gov.bt, tbtamang@nchm.gov.bt

Keywords: Flood frequency, trend, log-Normal and Log Pearson type III, return period, Man- Kendall, distribution

ABSTRACT

River flow trend analysis and flood frequency analysis study was carried out to understand historical flow trend and flood frequency of extreme events over the past years in the Punatsangchhu basin in central Bhutan. The flow data from Wangdirapids Hydrological Station on the Punatsangchhu River was used for the analysis.

The Man-Kendall test was performed at 5 % (0.05) significance level to identify the trend for the annual and seasonal flow: monsoon (JJAS) and winter (DJF) flows. The result showed linear trends but there is no statistically significant trend for the annual, monsoon and winter flows at Wangdirapids in Punatsangchhu.

The log-Normal and Log-Pearson III distributions were used for flood frequency analysis. The Log Pearson III distribution shows better fit and analyzed for return periods of 2, 5, 10, 50 and 100 years which yielded flow of 1263.07 cumecs, 1586.18 cumecs, 1850.54 cumecs, 2643.63 cumecs and 3054.87 cumecs respectively.

1. INTRODUCTION

Rivers are the main source of water for agriculture, environment sustenance and development of hydropower projects, which are main sources of revenue for the country. However, the country is highly vulnerable to flash floods and landslides due to heavy rainfall during the monsoon and GLOF (Glacial Lake Outburst Flood). Precarious geographical location and effects of climate variability have highly exposed Bhutan to a diversity of hazards such as cyclone induced storms, flash floods, landslide and GLOF(NCHM, 2019a).

GLOF events were experienced in the country in 1957, 1960, 1968 and 1994. It was reported that the 1994 GLOF event from Luggye Tsho killed 21 people, damaged 91 houses and 1,781 acres of land. The heavy rainfall brought by Cyclone Aila in 2009 caused Bhutan an estimated loss of US $ 17 million (NCHM, 2019a). The flood/flash floods are recurrent phenomenon in the country especially in summer when there is heavy rainfall.

There is no systematic record of flash floods in Bhutan but the reports in Kuensel since 1968 compiled by the National Center for Hydrology and Meteorology (NCHM, 2018) recorded more than 60 incidents of floods in different parts of the country. Flash floods took lives of several people and damaged properties, agricultural lands and important infrastructure like bridges, irrigation channels and mini-micro hydro power (NCHM, 2018).

The flood frequency analysis is one of the means of finding the number of occurrences and identification of the largest flood (Roy & De, 2015). The study of flood frequency is the basis for the analysis of flood control and mitigation projects including the design of many other projects(Roy & De, 2015).

Therefore, the study of the trend of historical flow data and also the frequency and magnitude of the floods in Bhutan is important. The study of long term trends in stream runoff is highly required for understanding implications of climate change on water resources in the Himalayan river basins(R.D Gupta, S.k Jain, 2014).

The current study intends to see the flow trend and frequency of extreme events over the past 28 years in the Punatsangchhu basin.

2. OBJECTIVE

The following are the main objectives of the study:

a. To study the river flow trend (1992-2019) and;
b. To analyze the flood magnitudes and flood frequency.

3. STUDYAREA

Punatsangchhu is one of the major river basins in Bhutan with Pho Chhu and Mo Chhu as the two major tributaries. Punatsangchhu has the highest number of Potentially Dangerous Glacial Lakes (PDGL) (9 in Pho Chhu and 2 in Mo Chhu) out of 17 in the head water(NCHM, 2019b), posing threats to the settlements and important structures located downstream. Wangdirapids station in Punatsangchhu has consistent time series flow data starting from 1992 to 2019.

Wangdirapids is located a few kilometers downstream from the Pho Chhu-Mo Chhu confluence (Fig. 1). The station falls under Wangduephorang Dzongkhag (District). It is located at 27.46º N latitude and 89.90º E longitude with an altitude of 1190 meters above sea level. It has a catchment area of 6271 square kilometers.

Wangdirapids station is categorized as a Principal hydrological station as per the record at National Centre for Hydrology and Meteorology, with advanced type of station equipped with staff gauges, cableway and winch shed and electronic water level recorder.

Figure 1*: Location of Wangdirapids station on Punatsangchhu basin*

4. DATA

Wangdirapids station's flow data from 1992 to 2019 (28 years) was used for the study. The descriptive statistics of the flow data was shown in **Table 1** below. The mean flow at the station is 294.06 cumecs, the highest flow recorded is 2650.26 cumecs in 2009 in the month of May while the minimum flow recorded is 51.71 cumecs in 2015 in the month of March.

The high variability in the flow with significant outliers recorded in 1994, 2009 and 2017, which was due to extreme rainfall events (**Figure 2**).

Table 1*: Descriptive Statistics of available historical flow data*

Statistics parameter	Flow (cumecs)
Mean	294.06
Standard Deviation	277.69
Coefficient of Variation	0.94
Minimum	51.71
Maximum	2650.26

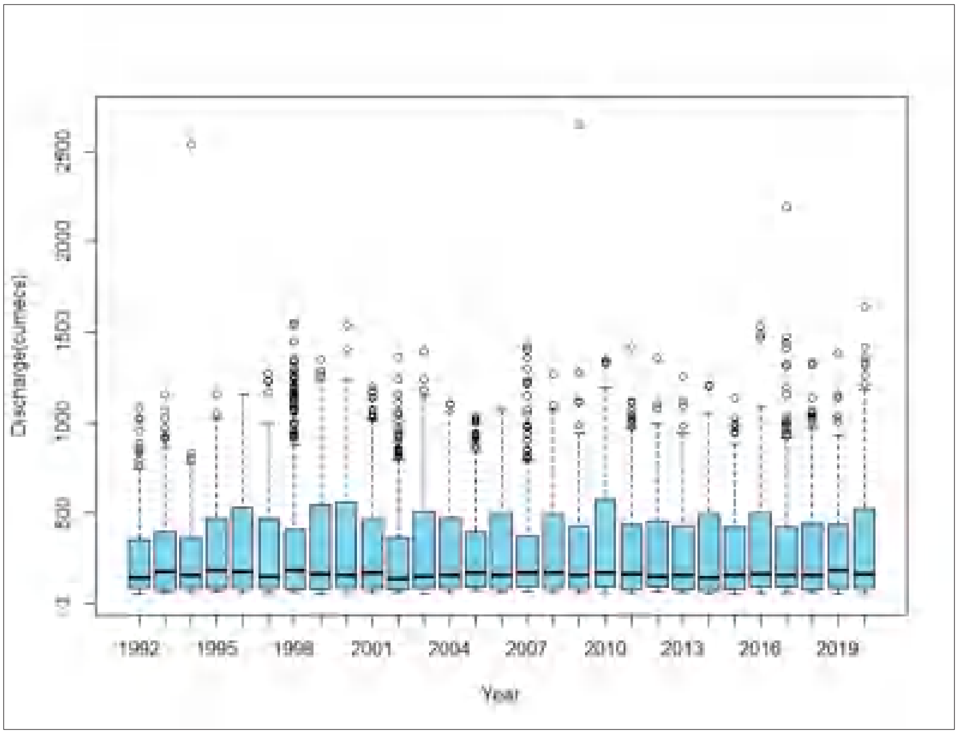

Figure 2*: Box plots for mean annual flow for each year*

5. METHODOLOGY

a) Trend Analysis

Analysis of Historical Climate and Climate projection for Bhutan revealed that the monsoon, June- September (JJAS) months are the wettest, whereas the December- February (DJF) are the dry winter season in Bhutan. The river flow in Bhutan follows rainfall seasonal pattern with peak flow in summer and lean flow in winter season. The flow trend analysis was carried out for annual, monsoon and lean/winter season. The mean annual flow, mean annual monsoon (JJAS) flow and mean annual lean (DJF) season flow were used during the analysis.

The non-parametric, Mann–Kendall was used to determine the trend in the flow data at 5 % statistical significance. The significance of Mann–Kendall test lies in its non-parametric nature, meaning the test doesn't assume any kind of distribution on the sample data, which also makes it more powerful test. The Mann–Kendall statistical test at 5 % significance level has been frequently used to test the significance of trends in hydro- meteorological time series (Bezak et al., 2016; da Silva et al., 2015).

The Mann-Kendall trend test was carried out using R software.

b) Flood Frequency Analysis

Log Pearson III and Log-Normal distributions were used for the flood frequency analysis. These techniques are most popular and common among the methods of flood frequency analysis (Garba & Tsoho, 2013; Krishan & Roy, 2016; Roy & De, 2015). The Log Pearson III and Log-Normal distributions were fitted for the annual peak flows using Hydrognomon4 software. Hydrognomon is an open source software tool used for the processing of hydrological data (Garba & Tsoho, 2013).

Kolmogorov-Smirnov (K-S) test is used to select the best distribution from the two. K-S is a goodness of fit test. The test checks how good the statistical distributions represent the observed data. The advantage of the K-S test is that it gives confidence interval in percent and provides a visual goodness-of -fit- test. The K-S test involves the comparison between the experimental cumulative frequency and the assumed theoretical distribution function (Garba & Tsoho, 2013).

Probability of exceeding/equaling the flood is calculated using the cumulative density function from the selected distribution. The probability values are then calculated into return periods in years (Return period=1/probability of exceeding/equaling the flood). For instance, if the flood has return period of 10 years, then it is concluded that the probability of exceeding or equaling that magnitude of flood is 1/10 (0.1) in any year.

The flood return periods of 2, 5, 10, 20, 50 and 100 years and flood frequency curves were calculated and plotted in excel.

6. RESULTS:

a) Trend Analysis Results:

The annual, monsoon and winter flows showed linear positive trends (Fig. 3-5). However, they are not statistically significant at 5 % significance level. The P values for all the three cases are observed to be greater than 0.05 (5 % significance level). P value represents the probability of the error (i.e. the possible trend due to inconsistent extremes or random fluctuation) when expecting that there is linear trend. So, higher the P value, lower the statistical significance and vice-versa. Therefore, the Man Kendall trend test indicates that there is no statistically significant linear positive trend at 5% significance level (**Table 2**).

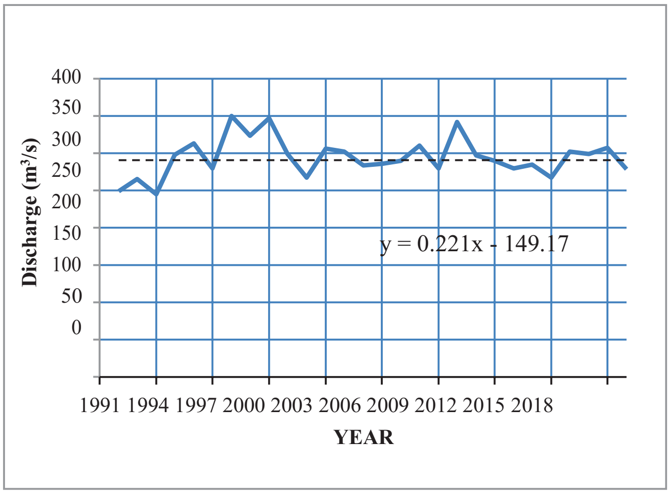

Figure 3*: Annual flow trend*

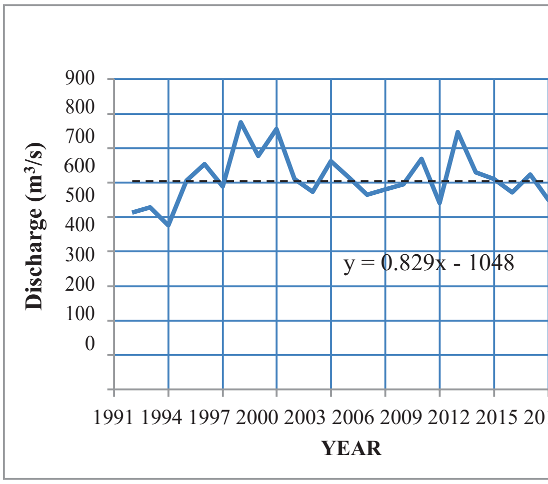

Figure 4: ***Monsoon (JJAS) flow trend***

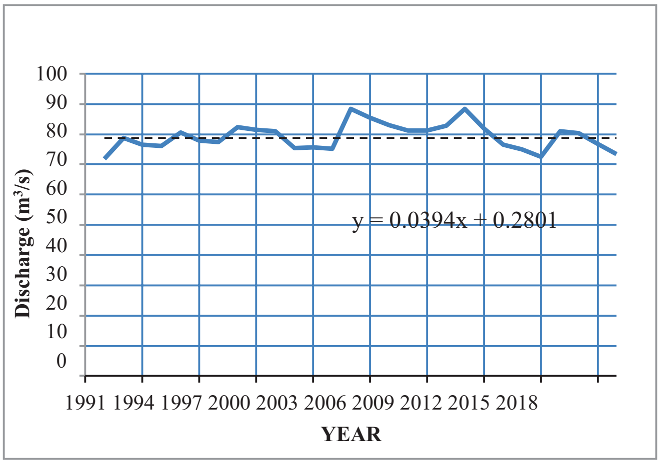

Figure 5*: Winter (DJF) flow trend*

Table 2*: Man-Kendall trend test result*

Scenario	**Mann-Kendall**	
	Kendall tau	p-value
Annual flow	0.003	0.83
Monsoon flow	0.08	0.54
Winter/lean flow	0.001	0.95

b) Flood Frequency Analysis Results:

The highest peak flow observed was on 25th May, 2009 with recorded 2650.26 m3/s of flow and lowest was observed on 25th July, 2006 with 1072.82 m3/s of flow (**Table 3**). Log-Pearson III and Log-Normal distributions are fitted to see which one better fits the peak flow data (**Figure 6**).

The Kolmogorov-Smirnov test shows that Log Pearson III fits best for the peak flow data at Wangdirapids. It was observed that the difference between observed values and the predicted cumulative values by both the distributions at level of significance of 1%, 5% and 10% been acceptable for both Log-Normal and Log Pearson III. But the Log Pearson III resulted in higher percentage of acceptance at all three significance levels (**Table 4**).

According to Log Pearson III distribution, the peak flows of 1263.07 m^3/s, 1586.18m^3/s, 1850.54 m^3/s, 2643.63m^3/s and 3054.87 m^3/s has return periods of 2, 5, 10, 50 and 100 years respectively (**Table 5**).

Table 3: ***Date of occurrence and magnitude of Peak flow***

Year	Peak Flow (m3/s)	Date of occurrence
1992	1089.13	25-Aug
1993	1155.47	08-Aug
1994	2539.19	07-Oct
1995	1154.89	30-Jun
1996	1158.54	13-Jul
1997	1274.02	18-Aug
1998	1550.74	02-Jul
1999	1355.43	24-Aug
2000	1541.33	20-Mar
2001	1202.91	19-Aug
2002	1364.71	20-Aug
2003	1395.45	08-Jul
2004	1105.85	07-Jul
2005	1034.04	15-Aug
2006	1072.82	25-Jul
2007	1424.38	31-Jul
2008	1265.29	22-Jul
2009	2650.26	26-May
2010	1345.59	23-Aug
2011	1420.71	20-Jul
2012	1359.88	25-Jul
2013	1256.81	22-Jul
2014	1209.25	15-Jul
2015	1138.87	20-Aug
2016	1532.61	26-Jul
2017	2195.30	10-Aug
2018	1329.94	01-Aug
2019	1386.74	05-Aug

Table 4*: Kolmogorov-Smirnov test result*

Kolmogorov-Smirnov test	a=1%	a=5%	a=10%	attained a
Log Normal	ACCEPT	ACCEPT	ACCEPT	22.16%
Log Pearson III	ACCEPT	ACCEPT	ACCEPT	94.44%

Table 5*: Flood Return period (in years) and probability of occurrence by Log Pearson III distribution*

Return Period(Years)	**Probability of occurrence**	**Log Pearson III**
2	0.5	1263.07
5	0.2	1586.18
10	0.1	1850.54
50	0.02	2643.63
100	0.01	3054.87

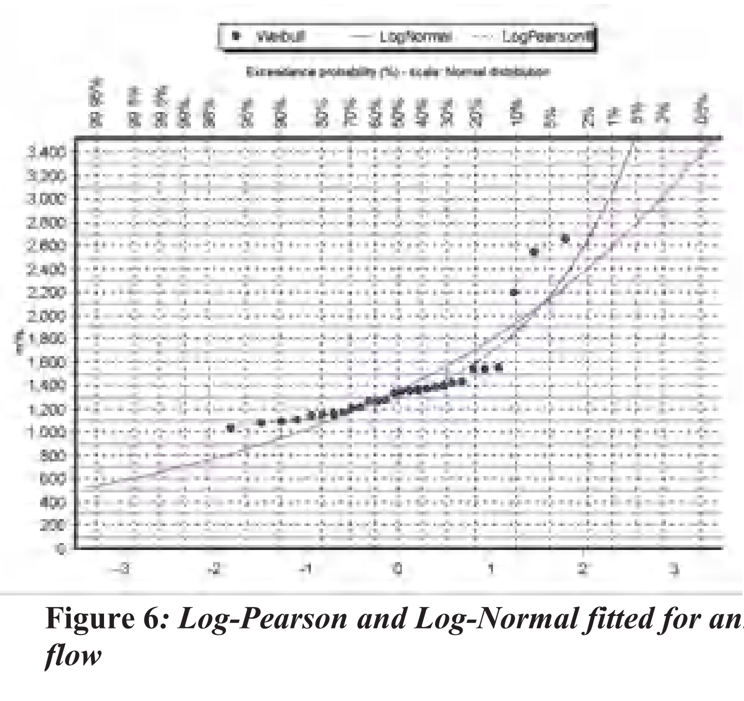

Figure 6*: Log-Pearson and Log-Normal fitted for annual peak flow*

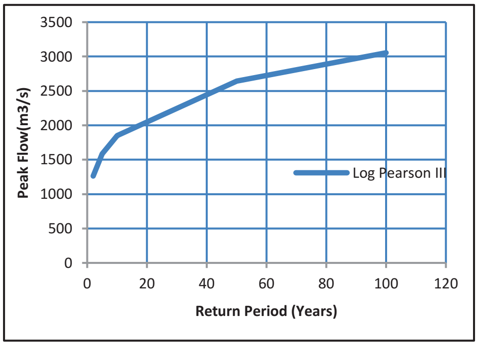

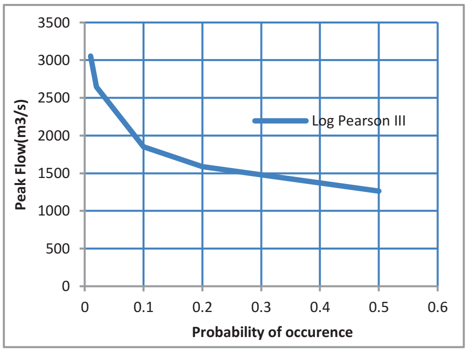

Figure 7*: Flood Frequency Curve and Probability of Occurrence curve*

7. CONCLUSION

Flow trend and flood frequency analysis is carried out for Punatsangchhu basin at Wangdirapids hydrological station with the objective to study the river flow trend and also to understand the frequency, magnitude and probability of occurrence of the extreme flood events during past 28 years.

The trend analysis observed that the flow at Wangdirapids station on Punatsangchhu is positive but the positive trend is statistically not significant at 5 % significance level. The linear positive trends observed might be contributed by the inconsistent extreme events and the in-significant trend might be due to the data period because studies of trend require a larger time period data of more than 30 years for better understanding and knowledge (R.D Gupta, S.k Jain, 2014).

Flood frequency analysis showed that the Log Pearson III distribution yielded better fit to the annual peak flows of Wangdirapids. There are several statistical distributions that are used while calculating return periods. The choice of distribution lies entirely to the river's flow pattern. Different distributions are suited to different flow patterns. As such, Log Pearson III was found best for the flow pattern at Wangdirapids. According to the best fitted distribution, the flow for each return period of 2,5,10, 50 and 100 years are 1263.07 cumecs, 1586.18 cumecs, 1850.54 cumecs, 2643.63 cumecs and 3054.87 cumecs respectively

Return period is the probability of occurrence of a flood in any given year. Understanding and knowing the probabilities of floods are of immense benefit while planning hydropower dams, bridges and construction of structures near the rivers. The return periods are also frequently used during the flood risk assessment while generating flood hazard maps.

References

Bezak, N., Brilly, M., & Šraj, M. (2016). Flood frequency analyses, statistical trends and seasonality analyses of discharge data: A case study of the Litija station on the Sava River. *Journal of Flood Risk Management*, *9*(2), 154–168. https://doi.org/10.1111/jfr3.12118

da Silva, R. M., Santos, C. A. G., Moreira, M., Corte-Real, J., Silva, V. C. L., & Medeiros, I. C. (2015). Rainfall and river flow trends using Mann–Kendall and Sen's slope estimator statistical tests in the Cobres River basin. *Natural Hazards*, *77*(2), 1205–1221. https://doi.org/10.1007/s11069-015-1644-7

Garba, H., & Tsoho, U. (2013). Fitting Probability Distribution Functions To Discharge Variability Of Kaduna River. *Ijmer*, *3*(5), 2848–2852. http://www.ijmer.com/papers/Vol3_Issue5/BM3528482852.pdf

Krishan, R., & Roy, L. B. (2016). Flood Frequency Analysis for Kosi River At Its Barrage Site. *Journal of Indian Water Resources*, *36*(1), 10–16.

NCHM. (2018). Compendium of Climate and Hydrological Extremes in Bhutan since 1968 from Kuensel. In *Compendium of Climate and Hydrological Extremes in Bhutan since 1968 from Kuensel*.

NCHM. (2019a). *Analysis of historical climate and climate projection for Bhutan. National Center for Hydrology and Meterology. Royal Government of Bhutan.*

NCHM. (2019b). Reassessment of Potentially Dangerous Glacial Lakes in Bhutan. National Center for Hydrology and Metereology. RGoB. In *Nchm*.

R.D Gupta, S.k Jain, D. S. (2014). Study of long term trend of river discharge of Sutlej river. *Geography Environment Sustainability*.

Roy, P., & De, S. K. (2015). a Comparative Approach To Flood Frequency Analysis of the Puthimari River in Assam, India. *Asian Journal of Spatial Science*, *3*(2347), 2347–7636.